

## Li Diffusion in Nano- and Microcrystalline $(1-x)\text{Li}_2\text{O}:x\text{B}_2\text{O}_3$

S. Indris<sup>1</sup>, P. Heitjans<sup>1</sup>, H.E. Roman<sup>2</sup> and A. Bunde<sup>3</sup>

<sup>1</sup> Institute for Physical Chemistry and Electrochemistry, University of Hannover, Callinstr. 3-3A,  
DE-30167 Hannover, Germany

<sup>2</sup> Sezione di Milano, I.N.F.N., Via Celoria 16, IT-20133 Milano, Italy

<sup>3</sup> Institut für Theoretische Physik III, Justus-Liebig-Universität Giessen, Heinrich-Buff-Ring 16,  
DE-35392 Giessen, Germany

**Keywords:** Ball Milling, Ceramics, Composites, Impedance Spectroscopy, Interfacial Regions, Ionic Conductor, Nanocrystalline Materials, NMR Spectroscopy

### Abstract

Li diffusion in nano- and microcrystalline  $(1-x)\text{Li}_2\text{O}:x\text{B}_2\text{O}_3$  composites was investigated with impedance and NMR spectroscopy in the temperature range from 140 K to 500 K. Impedance results for the nanocrystalline system differ drastically from those of the microcrystalline system and show an enhancement of the dc conductivity when adding the insulator  $\text{B}_2\text{O}_3$  to the ionic conductor  $\text{Li}_2\text{O}$ .  $^7\text{Li}$  NMR lineshape measurements confirm that this is due to an enhanced fraction of mobile ions in the interfacial regions between the conductor and the insulator. Activation energies obtained from the dc conductivity (0.95 eV) and the  $^7\text{Li}$  NMR relaxation rate  $T_1^{-1}$  (0.29 eV) are independent of the composition of the composites.

### Introduction

Nanocrystalline materials have a large fraction of grain boundaries [1,2] which can provide fast pathways for atomic diffusion [3-7]. Composite materials contain interfaces between different phases which can also show high diffusivity [8-13]. Combining both aspects we studied the nanocrystalline composite material  $(1-x)\text{Li}_2\text{O}:x\text{B}_2\text{O}_3$ . Mixing the Li conductor  $\text{Li}_2\text{O}$  with the insulator  $\text{B}_2\text{O}_3$  and subsequent compaction leads to a complex material with a network of different interfaces. Variation of the grain sizes and the composition allows us to model the network of the different diffusion pathways and to examine percolation of these pathways. We studied Li diffusion in the composite materials by impedance and NMR spectroscopy. The nanocrystalline components were prepared by ball milling and the insulator content  $x$  could be varied between 0 and 0.95. The grain size was varied between 10  $\mu\text{m}$  and 20 nm. Impedance measurements were performed in the frequency range from 5 Hz to 13 MHz and at temperatures between 300 K and 500 K. We found an increase of conductivity with insulator content  $x$  in the nanocrystalline composites whereas in the microcrystalline composites the conductivity decreases monotonically with  $x$ . In the nanocrystalline materials  $^7\text{Li}$  spin-lattice relaxation shows an increased rate compared to the microcrystalline samples and a slight deviation from single exponential behavior at temperatures above 370 K. The  $^7\text{Li}$  NMR lineshape exhibits two contributions which are attributed to the Li ions located in the grains and in the interfaces, respectively.

### Sample preparation and characterization

The nanocrystalline components  $\text{Li}_2\text{O}$  and  $\text{B}_2\text{O}_3$  were prepared separately by ball milling the microcrystalline source materials, which have an average grain size of about 10  $\mu\text{m}$  each. In contrast to other preparation techniques for nanocrystalline materials ball milling is suitable for

many materials, larger amounts can be produced and the average grain size can be controlled easily by variation of the milling time which is important to study grain size effects. We used a high-energy ball mill SPEX 8000 with an alumina vial and a ball-to-powder weight ratio of 2:1. The appropriate amounts of the two components were mixed and milled again for 15 minutes. Finally the powders were cold-pressed with an uniaxial pressure of 1 GPa to form the composites. XRD patterns did not show an indication for the formation of new compounds. The resulting pellets had a diameter of 8 mm and a thickness of typically 2 mm. The density was about 85% of the theoretical value. For comparison also microcrystalline composites were produced from the microcrystalline source materials (average grain size 10  $\mu\text{m}$ ) by mixing the appropriate amounts and compacting again under a pressure of 1 GPa. All preparation steps were done in argon atmosphere. The average grain size of the nanocrystalline samples was determined from the line broadening of XRD profiles using the method of Warren and Averbach [14]. The milling time was varied between 1 h and 16 h. The resulting average grain sizes range from 40 nm to 20 nm showing a saturation behavior for milling times longer than 4 hours [15]. These results are in good agreement with observations from transmission electron microscopy. The thermal stability of the samples was investigated with differential thermal analysis. It showed that grain growth starts at about 500 K. This could be verified by XRD line narrowing of the samples after exposure to this temperature for 10 hours.

### Impedance measurements

Impedance measurements were performed with a HP 4192A impedance analyzer using platinum electrodes. The frequency was varied between 5 Hz and 13 MHz at temperatures between 300 K and 500 K. For all samples the conductivity shows a plateau at lower frequencies and a dispersive region at higher frequencies. The dc conductivity  $\sigma_{\text{dc}}$  is extracted from the plateau and shows

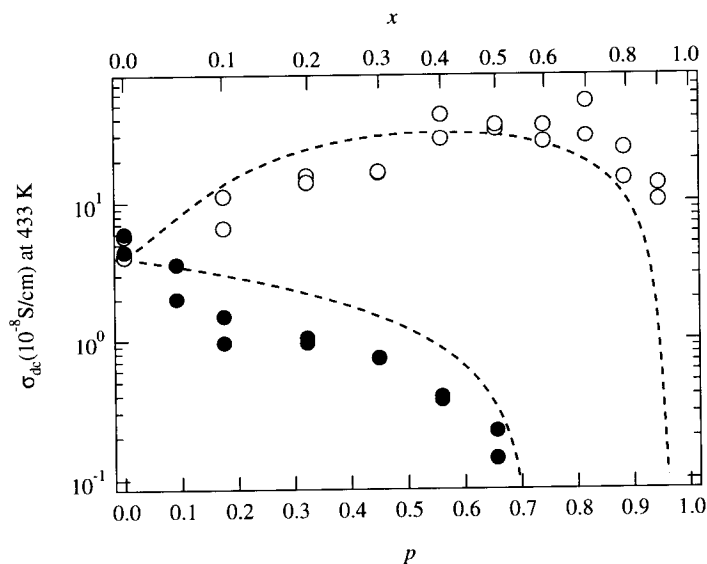


Figure 1: dc conductivities of the nanocrystalline (○) and microcrystalline (●)  $(1-x)\text{Li}_2\text{O}:x\text{B}_2\text{O}_3$  composites vs insulator volume fraction  $p$  and insulator mole fraction  $x$  (upper abscissa) at a temperature of 433 K. The dashed lines show results from continuum percolation theory [16].

Arrhenius behavior in the examined temperature range. The dc conductivity at 433 K is presented for different insulator volume fractions  $p$  in Fig. 1 for the micro- and nanocrystalline composites (the insulator volume fraction  $p$  is related to the insulator mole fraction  $x$  by  $p = \alpha x / (\alpha x - x + 1)$ , where  $\alpha = V_{\text{mol}}(\text{B}_2\text{O}_3) / V_{\text{mol}}(\text{Li}_2\text{O}) \approx 1.91$  is the ratio of the mole volumes). For pure  $\text{Li}_2\text{O}$  the dc conductivity is the same in the micro- and in the nanocrystalline sample. When adding the insulator the conductivity falls monotonically with  $x$  in the case of the microcrystalline material. In contrast to that in the nanocrystalline composites starting from  $x = 0$  the conductivity rises by a factor of about 10 up to a maximum at  $x \approx 0.5$ . Above certain thresholds ( $x \approx 0.55$  for the microcrystalline and  $x \approx 0.92$  for the nanocrystalline system) the dc conductivity falls drastically [16]. It is important to note that the activation energies are about 0.95 eV for all samples showing no significant dependence on the insulator content  $x$ . These results could be explained by a continuum percolation model [16]. It assumes that between the insulator grains and the grains of the ionic conductor a highly conducting interface does exist. The thickness of this interface is taken to be independent of the grain size. Results from this theory are shown in Fig. 1 as dashed lines. An enhancement in the conductivity was also found for the composite system  $\text{CuBr}:\text{TiO}_2$  with  $\text{CuBr}$  being microcrystalline and  $\text{TiO}_2$  being nanocrystalline and was explained with a discrete percolation model [13].

### NMR investigations

We measured the  $^7\text{Li}$  relaxation rate  $T_1^{-1}$  in the temperature range from 130 K to 500 K at frequencies between 19 MHz and 97 MHz. Results are shown in Fig. 2 for microcrystalline and nanocrystalline  $\text{Li}_2\text{O}$  at a frequency of 58 MHz. The measured relaxation rate consists,

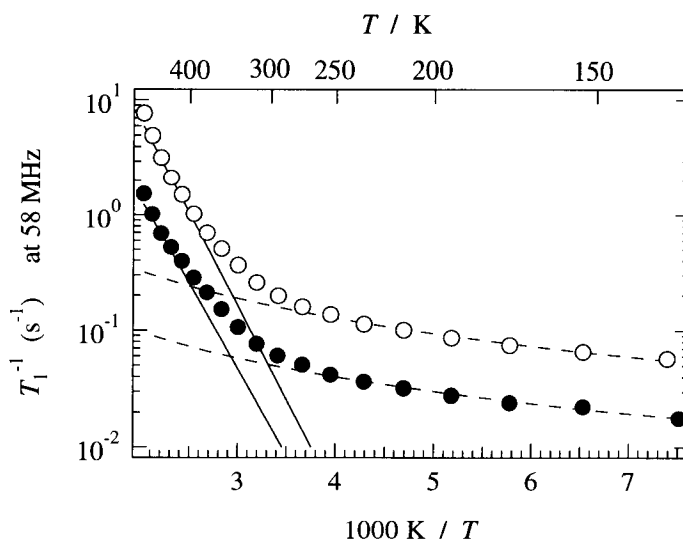


Figure 2:  $^7\text{Li}$  relaxation rates for micro- (●) and nanocrystalline (○)  $\text{Li}_2\text{O}$  at the frequency  $\nu = 58$  MHz. The dashed lines show the background contribution fitted with a power law  $T_1^{-1} \sim T^{-\gamma}$  yielding  $\gamma \approx 1.3$  and the solid lines show the Arrhenius behavior of the diffusion induced contribution to  $T_1^{-1}$  obtained after subtraction of the background contribution. The slopes yield activation energies of about 0.29 eV.

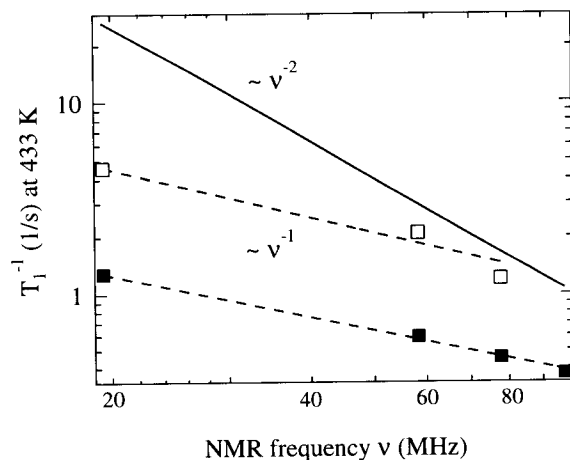


Figure 3: Frequency dependence of the  ${}^7\text{Li}$  relaxation rates of micro- (■) and nanocrystalline (□)  $\text{Li}_2\text{O}$  at 433 K. The solid line shows the result from standard BPP theory [17].

on the one hand, of a diffusion induced contribution which becomes dominant at  $T > 300$  K and rises to the typical  $T_1^{-1}$  peak. In the present case, due to grain growth above 500 K, only the low- $T$  flank is accessible. On the other hand, there is a background relaxation rate which is dominant at temperatures below 250 K and shows a weak temperature dependence. Assuming a power law this contribution was subtracted from the total rate yielding the purely diffusional contribution. The slope of the low- $T$  flank both for nano- and microcrystalline  $\text{Li}_2\text{O}$  yields an activation energy of about 0.29 eV. This can be attributed to the short-time behavior of the diffusion process, i.e. the elementary jumps, whereas the high- $T$  flank should give the activation energy for the long-time behavior, i.e. long-range diffusion [4]. The latter one should be equal to the value 0.95 eV found for the dc conductivity (see above). In the nanocrystalline material the flank is shifted to lower temperatures which indicates a highly increased jump rate. An additional effect may be an increase of the motion induced rate. This point is further to be examined by supplementary  ${}^6\text{Li}$  relaxation measurements. In both systems the relaxation rates and the activation energies reveal no significant dependence on the insulator content  $x$ .

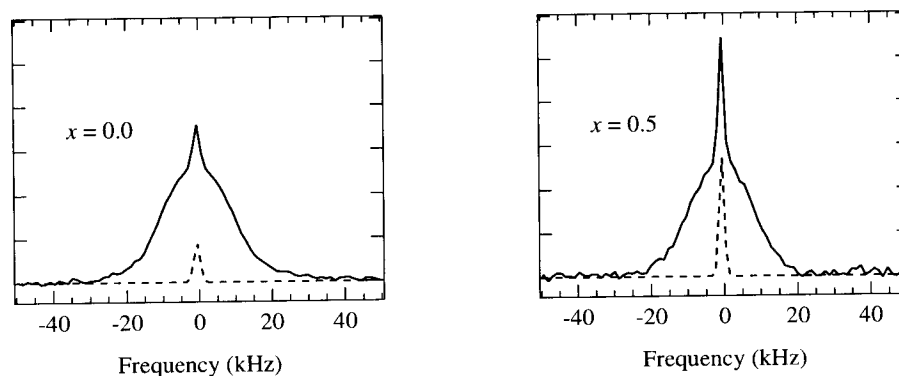


Figure 4:  ${}^7\text{Li}$  NMR lineshapes for the nanocrystalline composites with  $x = 0$  and  $x = 0.5$  at 433 K and a central frequency of 58 MHz. The dashed line shows the contribution of the motionally narrowed line.

Fig. 3 shows the frequency dependence of the relaxation rates for the microcrystalline and the nanocrystalline composites. The weak frequency dependence  $T_1^{-1} \sim \nu^{-1}$  instead of  $\nu^{-2}$ , which is predicted by the standard theory [17], yields evidence for strong correlations of the jumps of the ions [18]. We also studied  $^7\text{Li}$  NMR lineshapes in the temperature range from 130 K to 500 K. For temperatures below 330 K only one broad central line is visible. At higher temperatures a narrow peak on top of the broad line arises for the nanocrystalline materials. Fig. 4 shows the lineshape of two nanocrystalline composites with  $x = 0$  and  $x = 0.5$  at a temperature of 433 K and a frequency of 58 MHz. The lines clearly show two contributions in contrast to the microcrystalline samples where only one broad peak is visible. Both parts are separated by a fit with a sum of two Gaussian functions. The broader line has a width

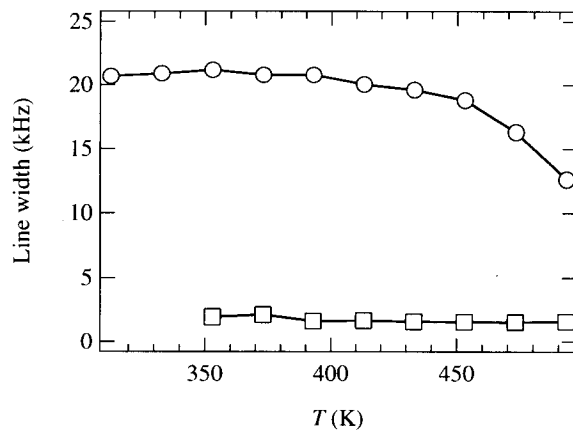


Figure 5:  $^7\text{Li}$  NMR line widths of the broad (○) and the narrow (□) part vs temperature for the nanocrystalline composite with  $x = 0$ . Results for  $x = 0.5$  are similar.

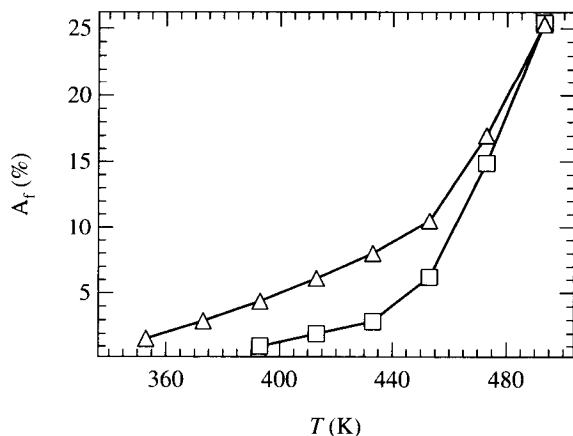


Figure 6: The fraction  $A_f$  of the narrowed line with respect to the total NMR line area vs temperature for two nanocrystalline composites with  $x = 0$  (□) and  $x = 0.5$  (△).

of about 20 kHz which is also found at lower temperatures. The same value is obtained in the coarse grained material and can thus be attributed to the immobile ions inside the grains. The narrow part which shows up at temperatures above 350 K can be ascribed to the mobile ions in the interfacial regions. Below this temperature, distinction of the two lithium species is not possible because the fraction of the narrow line is too small. Fig. 5 shows the line widths of the nanocrystalline composite for  $x = 0$  versus temperature. At  $T > 450$  K motional narrowing of the broad line, i.e. diffusion in the interior of the lithium oxide grains is starting. Above

500 K separation of the two lines is no longer possible because the line widths of the two lines become similar. Fig. 6 shows the fraction  $A_f$  of the narrowed line with respect to the total line area which yields the fraction of mobile ions. Below 450 K  $A_f$  is only determined by the mobile ions in the interfacial regions and strongly depends on  $x$ . Above 450 K also the ions in the grains become mobile (cf. Fig. 5) and  $A_f$  increases towards 100% irrespective of  $x$ . At 433 K, the temperature where the dc conductivity is measured, the fraction of fast diffusing lithium ions being located in the interfaces is estimated to be 3% in the composite with  $x = 0$  and 8% in the composite with  $x = 0.5$ . So the fraction of fast ions in the composite material is higher than in pure  $\text{Li}_2\text{O}$ . We conclude that the enhancement of the ionic conductivity with  $x$  is at least partly caused by an increase in the concentration of charge carriers whereas the diffusion barriers are not reduced.

## Conclusions

Impedance and NMR spectroscopy were employed to study diffusion in nanocrystalline ceramic composites on the complementary time scales of these methods. Evidence for fast diffusion in the interfacial regions was found by variation of the composition and the grain size of the heterogeneous materials. The impedance measurements show that diffusion is dominated by the boundaries between the ionic conductor and the insulator.  $^7\text{Li}$  NMR lineshape studies confirm that the mobile ions are located in these particular interfaces.  $^7\text{Li}$  NMR relaxation as well as the impedance measurements show no dependence of the activation energies on the composition. Furthermore the relaxation results indicate strongly correlated ionic motion.

## Acknowledgment

We are grateful to the Deutsche Forschungsgemeinschaft for financial support.

## References

- [1] H. Gleiter: *Progr. Mater. Science* **33** (1989), 223.
- [2] R. W. Siegel: *Encycl. of Applied Physics*, **11** (1994), 173.
- [3] I. Kaur, Y. Mishin and W. Gust: *Fundamentals of Grain and Interphase Boundary Diffusion*, John Wiley & Sons, New York (1995).
- [4] P. Heitjans and A. Schirmer, in *Diffusion in Condensed Matter* (J. Kärger, P. Heitjans, R. Haberlandt, eds.) Vieweg, Wiesbaden (1998), p. 116.
- [5] W. Puin and P. Heitjans: *Nanostruct. Mater.* **6** (1995), 885.
- [6] D. Bork and P. Heitjans: *J. Phys. Chem. B* **102** (1998), 7303.
- [7] W. Puin, S. Rodewald, R. Ramlau, P. Heitjans and J. Maier: *Solid State Ionics* **131** (2000), 159.
- [8] C. C. Liang: *J. Electrochem. Soc.* **120** (1973), 1289.
- [9] A. Bunde, W. Dieterich and H. E. Roman: *Phys. Rev. Lett.* **55** (1985), 5.
- [10] H. E. Roman, A. Bunde and W. Dieterich: *Phys. Rev. B* **34** (1986), 3439.
- [11] N. J. Dudney: *Ann. Rev. Mater. Sci.* **19** (1989), 113.
- [12] J. Maier, *Prog. Solid St. Chem.*, **23** (1995) 171.
- [13] J.-M. Debierre, P. Knauth and G. Albinet: *Appl. Phys. Lett.* **71** (1997), 1335.
- [14] B. E. Warren: *X-ray diffraction*, Addison-Wesley, Reading Massachusetts (1969).
- [15] S. Indris and P. Heitjans: *Mater. Sci. Forum* **343-346** (2000), 417.
- [16] S. Indris, P. Heitjans, H. E. Roman and A. Bunde: *Phys. Rev. Lett.* **84** (2000), 2889.
- [17] N. Bloembergen, E. Purcell and R. V. Pound: *Phys. Rev.* **73** (1948), 679.
- [18] K. Funke: *Prog. Solid. St. Chem.* **22** (1993), 111.